WHAT IS THE ROLE OF NUCLEAR EFFECTS IN ULTRARELATIVISTIC REACTIONS AT 158 GeV/NUCLEON?*

Andrzej Rybicki

The H. Niewodniczański Institute of Nuclear Physics, Polish Academy of Sciences
Radzikowskiego 152, 31-342 Kraków, Poland

(Received January 11, 2011)

In this paper I shall present a few simple examples on how the nuclear structure, nuclear density, isospin content, and finally the electric charge of the nucleus influence various aspects of multiparticle production in ultrarelativistic nuclear reactions.

DOI:10.5506/APhysPolB.42.867
PACS numbers: 25.75.–q, 12.38.Mh

1. Introduction

Taken most generally, two main motivations can be attributed to studies of ultrarelativistic nuclear reactions (by which, in this paper, hadron–nucleus and nucleus–nucleus collisions in the energy regime of a few or more GeV per incoming nucleon will be meant). On the one hand, it has been long believed that reactions more complex than the "elementary" hadron–hadron interactions can serve as a source of new information on the nature of the strong force in the non-perturbative sector of Quantum Chromodynamics (QCD). On the other hand, alternatively, studies of high energy nuclear collisions were driven by the hope of discovering new phenomena, not available from elementary reactions. Here one should in particular quote the hypothesis of Quark-Gluon Plasma formation in ultrarelativistic heavy ion collisions [1].

The fact that nuclear effects, and the characteristics of the atomic nucleus, play a role in nuclear reactions also in this high energy regime is probably not very surprising. It is nevertheless instructive to investigate how these effects manifest themselves in specific multiparticle production phenomena, and how important is their role for the understanding of the high energy reaction. This is the purpose of the present paper.

* Presented at the Zakopane Conference on Nuclear Physics "Extremes of the Nuclear Landscape", August 30–September 5, 2010, Zakopane, Poland.

2. Basic experimental issues

The principal phenomenon occurring in high energy elementary and nuclear collisions being the production of many new particles (mostly π mesons), the basic aim of the experiment is to reconstruct the final state particles outcoming from the collision, in terms of their full momentum vector as well as their identity (particle type). For the experimental data presented below, and originating from the NA49 fixed target experiment at the CERN SPS, the Time Projection Chamber (TPC) technique was used. Charged particles, passing through a system of four large TPC's, left ionization "tracks" in their effective gas volume. Dedicated techniques [2, 3] were then applied for momentum vector reconstruction as well as for particle identification via ionization energy loss (the dE/dx method). The particle spectra presented below were corrected for a number of experimental effects, including in particular the feed-down from weak decays (like, *e.g.*, $\Lambda \to p\pi^-$ or $K^0_{\rm s} \to \pi^+\pi^-$) into distributions of final state particles. A very detailed description of this problematics can be found in [3].

3. Nuclear density

The knowledge of the density distribution of the nucleons inside the nucleus plays a key role in ultrarelativistic nuclear collision studies as it is directly connected to all the estimates of the geometry, or "centrality" of the collision (see *e.g.* [4]), a parameter of basic importance for the interpretation of very numerous observed phenomena. This will be illustrated below by the example of a comparative analysis [5] of pion production in proton–proton ($p+p$) and proton–carbon ($p+\mathrm{C}$) interactions.

The inclusive longitudinal distributions of positively and negatively charged pions produced in inelastic $p+p$ and $p+\mathrm{C}$ collisions are shown in Fig. 1, panels (a) and (b), respectively. These are drawn as a function of the Feynman variable $x_{\rm F} = \frac{p_{\rm L}}{p_{\rm beam}}$, where $p_{\rm beam}$ is the momentum of the incoming proton beam, while $p_{\rm L}$ is the "longitudinal" momentum of the pion along the beam direction. Both quantities are defined in the nucleon–nucleon c.m.s.

A comparison of the two reactions is shown in Fig. 1 (c) where the ratio of the summed distributions, $R = \frac{dn/dx_{\rm F}{}^{p+\mathrm{C}}(\pi^+ + \pi^-)}{dn/dx_{\rm F}{}^{p+p}{}_{(\pi^+ + \pi^-)}}$, is drawn as a function of $x_{\rm F}$ (solid curve). The knowledge of the nuclear density distribution (deduced from the charge distribution of the ^{12}C nucleus [6] shown in Fig. 1 (d)) allows for a further, quantitative analysis of the $x_{\rm F}$-dependence of this ratio. Assuming that the high energy projectile proton follows a straight line path through the target carbon nucleus with the inelastic interaction cross-section known from $p+p$ collisions, Fig. 1 (e), the probability that it will collide with

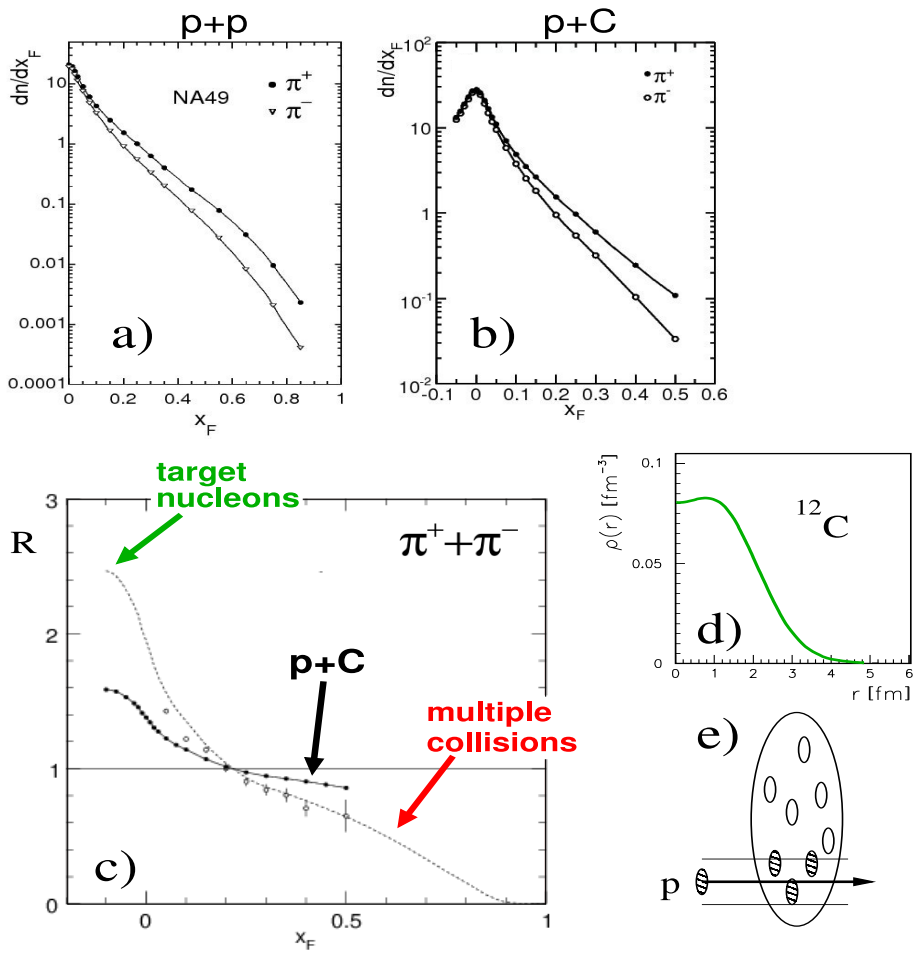

Fig. 1. (a), (b) Longitudinal distributions of positive and negative pions produced in inclusive inelastic $p + p$ [3] and $p + \mathrm{C}$ [7] reactions at 158 GeV beam energy. (c) Ratio of summed charged pion production in inclusive inelastic $p + \mathrm{C}$ relative to $p + p$ collisions (solid), compared to the same ratio extracted for $p + \mathrm{C}$ reactions where the projectile proton collides more than once (dashed). The latter ratio is superimposed with the same quantity obtained for $p + \mathrm{C}$ events leaving a minimum of two grey tracks in the NA49 detector (open circles); the plot is redrawn from [5]. (d) Charge density distribution for the $^{12}\mathrm{C}$ nucleus, drawn on the basis of [6]. (e) Schematic sketch of the $p + \mathrm{C}$ reaction.

only one target nucleon can be estimated (see [1,4]). Such a proton–nucleon collision being presumably similar to that known from $p + p$ data, this single collision contribution can be subtracted from the ratio R.

What comes out is the ratio corresponding to $p + \mathrm{C}$ reactions where the projectile collides *more than once*, shown as the dashed curve in Fig. 1 (c). This is characterized by a very steep x_F-dependence, which however can be readily interpreted. The accumulation of pions in the target c.m.s. hemisphere of the reaction ($x_\mathrm{F} < 0$) corresponds to the presence of relatively numerous target (carbon) nucleons, Fig. 1 (e), each of them contributing to pion production. In the projectile fragmentation region at large positive x_F, a strong depletion of pion yield is present, which is apparently induced by the multiple collisions of the projectile in the nucleus.

The above phenomenological study of the multiple collision process could also be verified experimentally [7]. The measurement of $p + \mathrm{C}$ events with at least two "grey" protons observed with low lab energy (open circles in Fig. 1 (c)) also suppresses the presence of single collisions [5] and comes into agreement with the dashed curve.

4. Isospin

In high energy reactions where many new particles are created, it might seem at first sight that the isospin of the incoming primary particles would play a negligible role. This is not true at SPS energies. Fig. 2 (a) shows the x_F-dependence of the ratio of produced π^+ over π^- densities in $p + p$ collisions. The π^+/π^- ratio increases with x_F, coming close to a factor of two at $x_\mathrm{F} = 0.3$. This is compared to the inverse (π^-/π^+) ratio in $n+p$ reactions. Taking into account the relatively low statistics and the preliminary status of the $n + p$ measurement [8], one can nevertheless conclude that the two

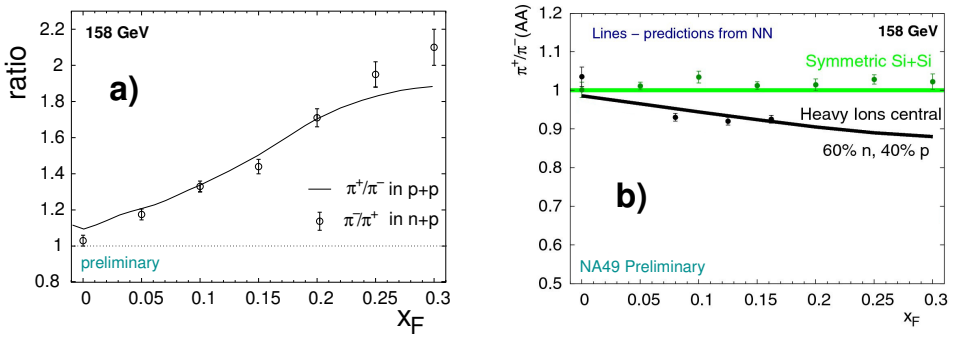

Fig. 2. (a) Ratio of produced π^+/π^- in $p + p$ collisions at 158 GeV beam energy, compared to the π^-/π^+ ratio in $n + p$ reactions. The curve is an interpolation of NA49 data [3], redrawn from [5]. The data points are redrawn from [8]. (b) π^+/π^- ratio in $\mathrm{Si} + \mathrm{Si}$ and central Heavy Ion ($\mathrm{Pb} + \mathrm{Pb}$) reactions at 158 GeV/nucleon beam energy, compared to predictions described in the text. The plot is redrawn from [8].

ratios come close at positive x_F, that is, in the fragmentation region of the projectile (proton in $p + p$ and neutron in $n + p$ collisions). This can be regarded as a direct consequence of isospin symmetry.

On the basis of this knowledge on the fragmentation of both proton and neutron into π^+ and π^- mesons, a prediction for any superposition of colliding protons and neutrons can be constructed. In particular, this is shown in Fig. 1 (b) for two types of nucleus–nucleus reactions. For the symmetric case of Si + Si collisions (50% protons over 50% neutrons), the prediction trivially corresponds to unity. For Pb + Pb reactions (40% protons over 60% neutrons), the prevalence of neutrons reflects in a moderate decrease of the π^+/π^- ratio with x_F. In both cases, the predicted trend comes close to the results of a preliminary analysis of Si + Si and central Heavy Ion (Pb + Pb) collisions [8]. It can therefore be concluded that the process of fast charged pion production at SPS energies preserves the "memory" of the isospin content of the incoming nucleus, and can be at least to first order understood on the basis of elementary interactions.

5. Nuclear charge

5.1. Peripheral Pb + Pb collisions

This section will address the problem of the influence which the nuclear charge exerts on final state spectra of particles produced in peripheral Pb + Pb collisions at 158 GeV/nucleon beam energy. By "peripheral", this paper will define collisions occurring at a relatively large impact parameter, comparable to twice the root-mean-square radius of the incoming Pb nuclei. Due to the relatively small geometrical overlap, such collisions correspond only to several tens of nucleons directly participating in the reaction ("participants" or "wounded nucleons" [9]). The remnants of the two nuclei are known as "spectator systems"; they inherit the bulk of the nuclear charge.

The small number of participating nucleons results in the production of a relatively moderate number of particles if compared to central Pb + Pb reactions. The experimental sample of peripheral Pb + Pb collisions discussed here was isolated by a cut on 150–300 charged particles seen in the NA49 detector, to be compared to up to 1500 in most central Pb + Pb reactions [10].

Fig. 3 (a) shows the experimental data on the π^+/π^- ratio in peripheral Pb + Pb reactions, drawn as a function of x_F in fixed bins of the "transverse" momentum p_T (*i.e.*, the pion momentum component perpendicular to the beam axis). At higher values of p_T, the π^+/π^- ratio displays a smooth decrease with x_F, see Fig. 2 (b) for comparison. However, a dramatic drop of this ratio is present at low transverse momenta. Here the ratio comes close to zero in the vicinity of $x_F = 0.15 \approx \frac{m_\pi}{m_N}$, which corresponds to pions moving longitudinally at spectator velocity [10]. Account taken of the

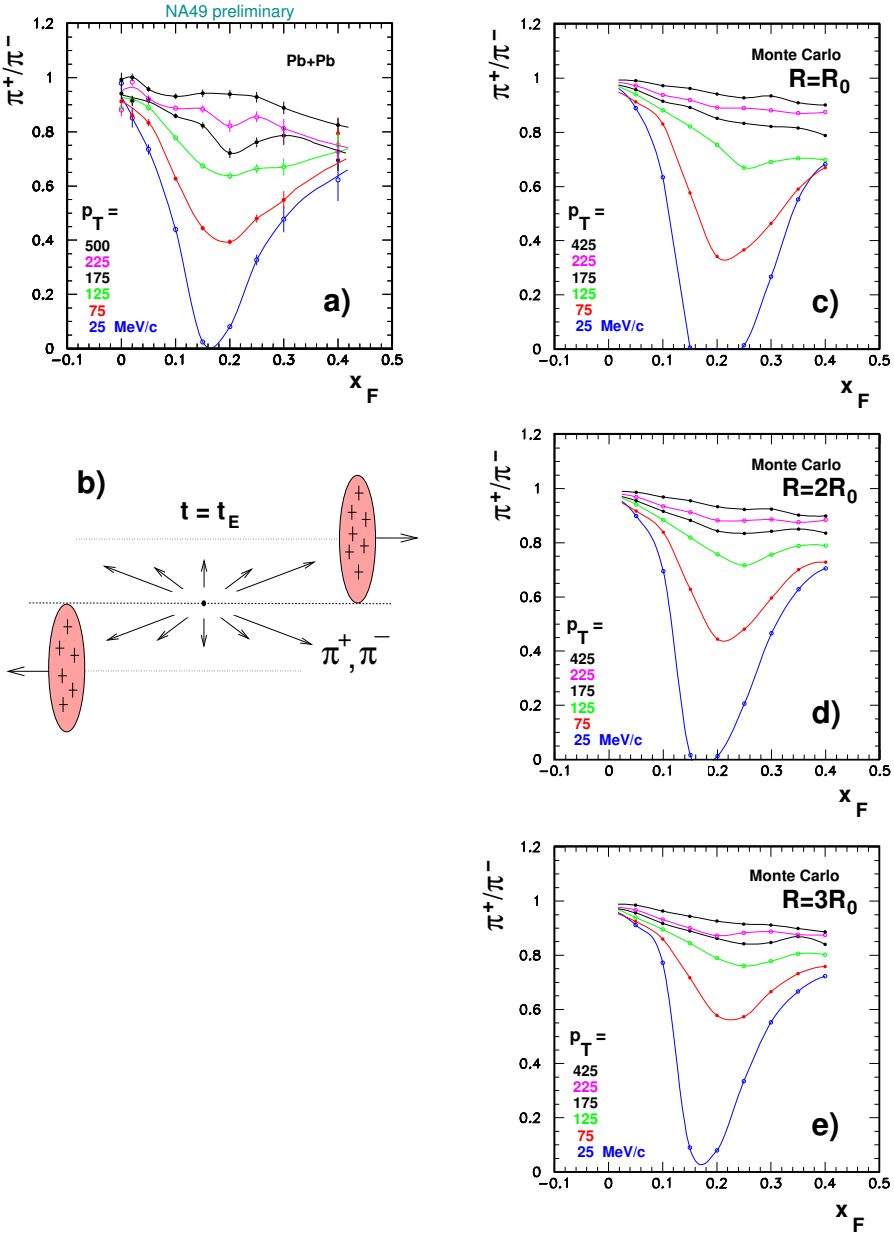

Fig. 3. (a) π^+/π^- ratio measured in peripheral Pb + Pb reactions [10], drawn as a function of x_F at fixed values of p_T (listed from top to bottom curve). (b) Model of the peripheral Pb + Pb reaction [11]. (c) Result of the simulation described in Sec. 5.2 [10]. (d), (e) Results of the simulation described in Sec. 5.3.

mixed proton/neutron content of the Pb nucleus, Sec. 4, such a low value for the π^+/π^- ratio suggests that the responsible for this effect would not be the strong interaction, but rather another force, not constrained by isospin symmetry. A natural candidate is the *electromagnetic interaction* induced by the presence of the spectator charge. This results in the repulsion of positive pions away from spectator vicinity and, at the same time, attraction of negative pions.

5.2. The electromagnetic distortion and its dependence on initial conditions

In order to quantify the hypothesis presented above, a theoretical study was performed. This was based on a simplified model of the peripheral Pb + Pb reaction [10, 11], shown schematically in Fig. 3 (b). The two outgoing spectator systems were modeled as two Lorentz-contracted, uniformly charged spheres. The sphere radius R_0 was defined by its standard nuclear density, $\rho = 0.17/\mathrm{fm}^3$. Charged pion emission took place from a single point in space, namely the original interaction point, and after a given emission time t_E. The model took account of isospin effects which were estimated on a similar basis as in Sec. 4, from experimental data on elementary interactions [3]. After the propagation of charged pions through the spectators' electromagnetic field, the result of the simulation is shown in Fig. 3 (c). Evidently, a reasonable description of the main characteristics of the data is obtained.

An important feature of the above electromagnetic effect is its dependence on the initial conditions imposed on the process of pion emission. This issue was studied with a slightly simpler version of the model described above (see [11] for an in-depth discussion of the corresponding details). Fig. 4 (left panels) shows the electromagnetic distortion of π^+/π^- ratios, obtained for different assumed values of the pion emission time t_E. These are now drawn in the full range of x_F, $-1 < x_\mathrm{F} < 1$, and for different values of p_T. The effect appears clearly sensitive to t_E. With increasing emission time, the position of the "valley" seen in the data in Fig. 3 (a) slowly moves towards higher values of x_F, and simultaneously, a decrease of the π^+/π^- ratio at large x_F is apparent[1]. In other terms, *the electromagnetic distortion of charged pion spectra depends on the space-time scenario imposed on pion emission.* This implies that it could provide independent information on the evolution of the non-perturbative process of pion production in space and time [10, 11].

[1] Note: the two "valleys" symmetric with respect to $x_\mathrm{F} = 0$, seen in Fig. 4 evidently correspond to the two spectator systems from the projectile and target nucleus.

5.3. Fragmentation of the spectator system

The studies discussed up to now neglected the problem of nuclear fragmentation of the spectator system. It is however clear that generally, the spectator nuclear remnant will not remain a stable sphere as postulated in Sec. 5.2, but will subsequently break-up into nuclear fragments as well as single nucleons [1]. A simple analysis was performed to investigate this problem. Instead of assuming the spectator system as a sphere at its original size and density, see above, the simulation was made assuming the spectators' sphere radius increased by a factor of two ($R = 2R_0$) and by a factor of three ($R = 3R_0$), together with the corresponding decrease of its density. The results of this simulation are shown in Figs. 3 (d) and 3 (e). Compared to the primary simulation from Fig. 3 (c), expanding the spheres' radius clearly improves the agreement with the experimental data from Fig. 3 (a), in particular in the vicinity of $x_{\mathrm{F}} \approx 0.2$, low p_{T} where the primary simulation visibly overpredicted the magnitude of the electromagnetic effect. On that basis, we can postulate that charged pions moving in the electromagnetic field of the spectator system "see it" not as a stable sphere, but rather as an expanding object. Thus, the electromagnetic distortion would appear sensitive to the process of spectator fragmentation, and could provide new information on the space-time evolution of this phenomenon.

5.4. Kaons

Strange particles are known to play an important role in heavy ion collision studies because the enhancement of strangeness production relative to elementary reactions is postulated as a signature of Quark-Gluon Plasma formation [1]. It is therefore natural to extend the studies discussed in the precedent sections to the domain of strange meson (K^+, K^-) production. This was made on the basis of a model similar to that described in Sec. 5.2. The principal difficulty here was the evaluation of realistic initial spectra for the emitted kaons over the full available range of x_{F}. These were constructed on the general basis of existing experimental data on kaon production in Pb + Pb collisions [12], supplemented with information from $p+p$ reactions [13] at high x_{F}. The details of this procedure are left for a separate publication. The resulting prediction for the electromagnetic distortion of the K^+/K^- ratio is shown in Fig. 4 (right panels) for two values of the kaon emission time t_{E}.

As visible from the figure, the electromagnetic field induced by the presence of spectators strongly influences the shape of final state kaon spectra, in particular at lower values of p_{T} and large x_{F} where a broad and deep valley in the K^+/K^- ratio is predicted. This effect superimposes on purely hadronic (or nuclear) phenomena which also influence this ratio [12, 13]. With an at

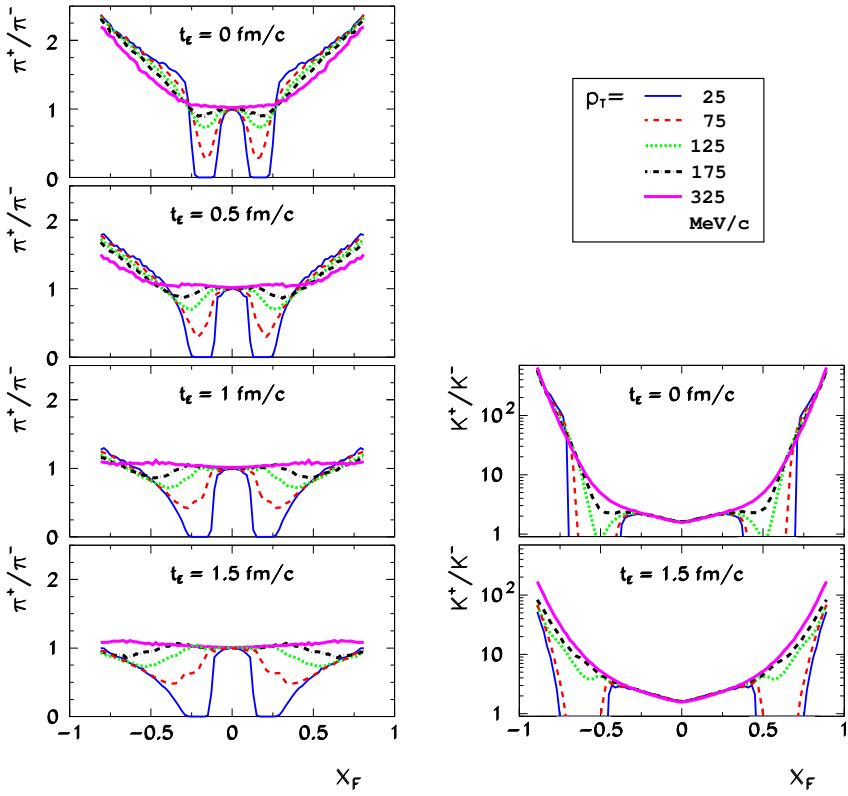

Fig. 4. Dependence of the electromagnetic distortion of π^+/π^- (left) and K^+/K^- (right) ratios, for particles produced in peripheral Pb + Pb collisions. The different panels correspond to different pion and kaon emission times t_E. The left panels are redrawn from [11].

least qualitative similarity to the case of pions from the left panels of Fig. 4, the effect for kaons exhibits some sensitivity to initial conditions: increasing the emission time results in a change of the position and shape of the valley mentioned above. Also, at high x_F ($x_F > 0.75$), the K^+/K^- ratio decreases with increasing t_E. As such, it can possibly provide information on space-time evolution of the reaction. It should however be underlined that relative to pions, the region of highest sensitivity is displaced towards much higher values of x_F.

6. Summary

The discussion made in this paper shows that the structure of the nucleus, its isospin content, and finally the nuclear charge leave a strong imprint on phenomena occurring in non-perturbative particle production in

ultrarelativistic nuclear collisions at 158 GeV/nucleon. As it appears, this brings important insight into various aspects of such reactions, in particular multiple collisions, particle production ratios, or the space-time evolution of the non-perturbative particle production process. These and other examples point at the importance of the knowledge obtained in the domain of nuclear physics for our understanding of the strong interaction in the high energy regime.

I wish to thank all the organizers of the Zakopane Conference on Nuclear Physics for their kind invitation. I also wish to thank numerous participants for the interesting remarks and questions which I received after presenting these results; some of these I tried to address in the present article. I wish to acknowledge the very important role of H.G. Fischer, M. Makariev, D. Varga and O. Chvála in the various experimental works discussed here, and obtained within the framework of the NA49 Collaboration. I also wish to underline the very important contribution of A. Szczurek to all the theoretical studies presented above. This work was supported by the Polish Ministry of Science and Higher Education under grant no. N N202 078735.

REFERENCES

[1] For a comprehensive description of these issues, see *e.g.*: J. Bartke, *Introduction to Relativistic Heavy Ion Physics*, Hackensack, USA: World Scientific, 2009 and references therein.

[2] [NA49 Collaboration] S. Afanasiev *et al.*, *Nucl. Instrum. Methods* **A430**, 210 (1999).

[3] [NA49 Collaboration] C. Alt *et al.*, *Eur. Phys. J.* **C45**, 343 (2006).

[4] A. Rybicki, Report No. 1976/PH, H. Niewodniczański Institute of Nuclear Physics, Polish Academy of Sciences, Kraków 2006.

[5] G. Barr *et al.*, *Eur. Phys. J.* **C49**, 919 (2007) and references therein.

[6] E.A.J.M. Offermann *et al.*, *Phys. Rev.* **C44**, 1096 (1991).

[7] [NA49 Collaboration] C. Alt *et al.*, *Eur. Phys. J.* **C49**, 897 (2007).

[8] [NA49 Collaboration] O. Chvála, *Eur. Phys. J.* **C33**, S615 (2004) and references therein.

[9] A. Białas, M. Bleszyński, W. Czyż, *Nucl. Phys.* **B111**, 461 (1976).

[10] A. Rybicki, *PoS* **EPS-HEP2009**, 031 (2009).

[11] A. Rybicki, A. Szczurek, *Phys. Rev.* **C75**, 054903 (2007).

[12] [NA49 Collaboration] S.V. Afanasiev *et al.*, *Phys. Rev.* **C66**, 054902 (2002); [NA49 Collaboration] C. Alt *et al.*, *Phys. Rev.* **C77**, 034906 (2008).

[13] J. Singh *et al.*, *Nucl. Phys.* **B140**, 189 (1978); A.E. Brenner *et al.*, *Phys. Rev.* **D26**, 1497 (1982); [NA49 Collaboration] T. Anticic *et al.*, *Eur. Phys. J.* **C68**, 1 (2010) and references therein.